LA-UR-21-28780
Approved for public release; distribution is unlimited.

Title: Air Blast Mesh Sensitivity and Pressure Mapping Study

Author(s): Vander Wiel, Gerrit Alan
Rutherford, Paula Anne
Wolfram, Phillip Justin Jr.

Intended for: Report

Issued: 2021-09-03

Air Blast Mesh Sensitivity and Pressure Mapping Study

August 11, 2021

Los Alamos National Laboratory: W-13 Advanced Engineering Analysis

Author: Gerrit Vander Wiel

Mentors: Paula Rutherford & Phillip Wolfram

Abstract:

Nose cone structural and aerodynamic characteristics are essential for intelligent design of aircraft, spacecraft, and ballistic systems. Finite element analysis can be used to help understand the structural integrity and flight characteristics of different nose cones. A mesh sensitivity study was undertaken for a particular nose cone geometry that was used in tests at LANL facilities in order to confirm the integrity of the meshed geometry. A simple cone that best matched closed-form theoretical solutions was modeled, and received good correlation to the theory. Complexity was then added back to the nose cone. Parameters applied to the simple cone were then implemented in the nose cone geometry giving assurance of accuracy after the geometry was changed. Nose cone results averaged 6.3% error for radial displacement when compared with the theoretical. Hoop stress averaged 6.0% error and meridional stress averaged 5.7% error at the finest mesh level. Meshes showed signs of convergence when compared to all three theoretical solutions. Finally, pressure time-history data from LANL computational fluid dynamics simulations was applied to the surface of the final nose cone geometry. The pressure data was interpolated from pressure gauge locations onto nearby meshed elements, which allowed for FEA software to run simulations on the cone with the pressure data as a loading condition. The pressure mapping resulted in the ability to understand the nose cone's rigid body motion that in turn can inform design of future nose cones.

Introduction:

Many objects are designed to travel through fluids. One of the most common instances of this is an object designed to glide through the air such as the nose of an aircraft, spacecraft reentry body, or a bullet. All of these objects are formed with similar aerodynamic profiles that help them perform efficiently, with the desired structural integrity and control characteristics. In order to be designed intelligently, the characteristics of each nose cone must be understood in terms such as internal stresses, external pressure loading, and the rigid body responses. One method for understanding how design affects these responses is through finite element analysis.

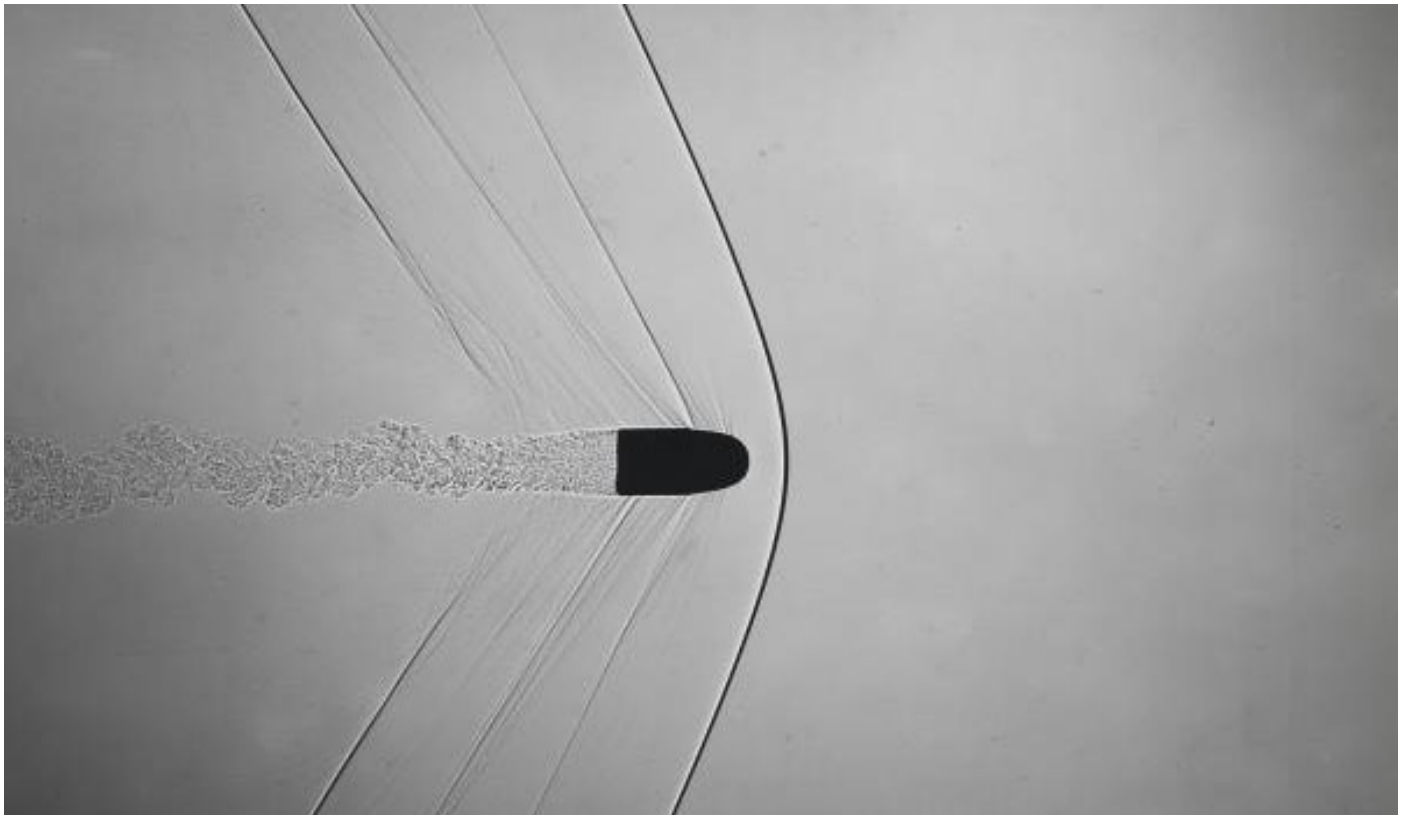

Figure 1 Shadowgraph captures a bullet traveling through a gelatin medium. A pressure wave is depicted at the fore, and turbulence at the rear.

(Bullet Shock Wave, Artist: Herold E. Edgerton, Smithsonian American Art Museum)

Ideally, analysts would be able to find closed form solutions for every model, however this is simply not the case. Only the simplest of geometries have analytical solutions hence the need for other methods of numerically calculating how geometries react to varied environments. Because a perfect solution is not always achievable, methods for achieving the best possible solution need to be analyzed in hope that concepts from one study can be applied to the next problem.

Project Goals:

This particular study focused on building a nose cone geometry and understanding certain characteristics about it. Particular attention was given to characteristics such as internal stresses experienced by the body, external pressures experienced by the body, and how the body would react to applied external pressures. The finite element analysis tool Abaqus was used to help determine how the geometry would react in varied environments. The nose cone geometry had been utilized in physical tests that were meant to model how conic bodies behave in blast environments.

There were two main goals for the research. First, to conduct a mesh sensitivity study. This study would provide confidence that the finite element model would react in a physically to applied conditions. Ensuring that the model was reacting in a physical manner required confidence that loads, boundary conditions, and material properties all represented something beyond the virtual model, which could be replicated in the physical world. These characteristics were to be confirmed by finding a mesh density at which the results started to converge, and also to build a model that reflected theoretical, closed-form solutions.

The second goal of the research was to understand how external pressure affected the nose cone, once confidence had been gained that the nose cone would react in a physical manner. Pressure was to be mapped onto the surface of the nose cone using experimental pressure time-history data. By mapping the pressure time-history the Abaqus finite element solver would be able to provide analysis data on how the body reacted in terms of rigid body motion such as acceleration and velocity, as well as what internal stresses the body experienced from external, non-uniform loading.

Model Definitions:

The conic body referenced previously had been already been built for physical tests gathering data on how the cone would react. Included in this geometry package were a myriad of sensors, gauges and other complexities in geometry. In modeling the test piece, nearly all of the complexities were excluded. Pressure gauge locations were mapped to the external surface of the modeled cone as nodes, which would be later required for the pressure mapping.

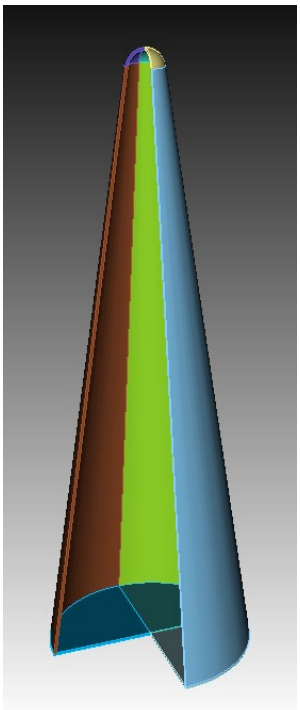

Figure 3 Geometry built in CUBIT

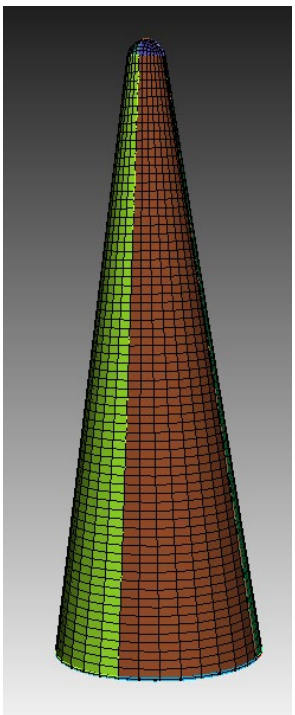

Figure 2 Geometry meshed in CUBIT

Simplifications in the model included a uniform 0.25 inch thickness throughout the entire model. This excluded many of the geometric complexities, and would be best suited for conducting the following mesh sensitivity study. All of the external surfaces were modeled exactly as the drawing package described, in a CAD and meshing software called CUBIT. CUBIT software provides certain Python capabilities that allow for programmatically changing parameters in geometry and meshing. The CUBIT Python interface was the method for translating the gauge locations from the engineering drawing package into Cartesian coordinates that could be mapped onto the surface of the nose cone.

Mesh Sensitivity:

A mesh sensitivity study was conducted in order to find parameters that best described a physical model and determine at what mesh density the model began to converge. One of the hopes was to model a simple geometry, confirm its accuracy, then add complexity back over time. Understanding mesh sensitivity is also important when considering the computational and analyst time for the cost of a simulation. In other words, more complex models use more computational power, so an optimal mesh density being decided would both ensure that the cost is not too high, and that the results will be valuable. One way of confirming adherence to real world phenomena was to compare model results to a theoretical solution. The other was to confirm that the simulation results converged at high mesh densities.

Theoretical solution

Because the model geometry was greatly simplified, a theoretical solution was chosen that seemed to best mirror the geometry of the nose cone. The solutions came from a study written for the DOD in 1964 that described vessels undergoing internal pressures (Norman Au, 1964). The vessels were then described in terms of stresses and displacements in the material.

The pressure vessel used for comparison with the nose cone was a simple, thin walled cone loaded with an internal pressure. The key difference between the model geometry and the theoretical geometry was the tip of the cone. The model nose cone included a semi-spherical blunt tipped nose, whereas the theoretical solution included a tip that converged to a singular point (Figure 4).

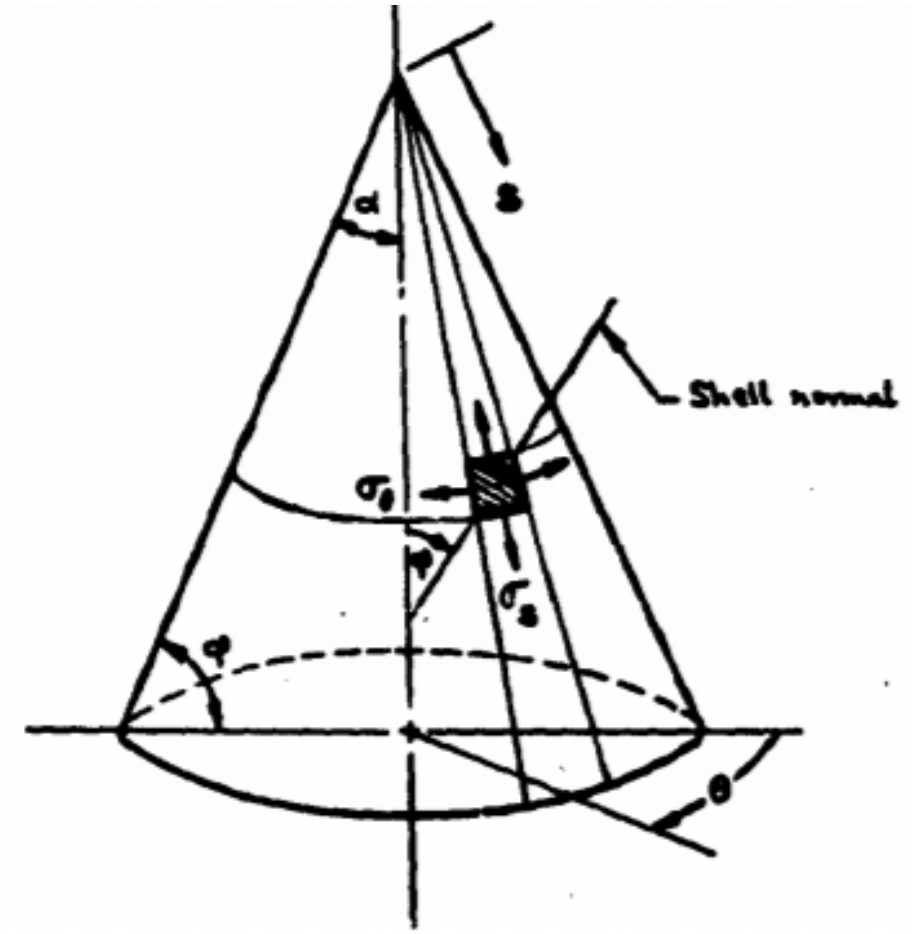

Figure 4 Diagram with theoretical conic pressure vessel

The report described the pressure vessel as "a container that must withstand an internal pressure, and is in the form of a surface of revolution with a wall thickness small compared to the radii of curvature of the wall (h/a ≤ 1/15)." (Au 1). Noting that *h* is the thickness of the conic body and *a* is the angle shown above between the outer surface and the cones center line.

The nose cone that was modeled in CUBIT met these requirements and was indeed considered a thin shell:

$$\frac{h}{a} = 0.03 \rightarrow (0.03 \leq 0.067)$$

Other assumptions were that the body had to be perfectly elastic, homogenous and isotropic. It had to have a uniform thickness and the only loading was from internal pressures meaning that all loading that the weight of the object could contribute was neglected (Au 2).

The thin walled pressure vessels were then assigned analytical solutions for hoop stress, meridional stress, and radial displacement. :

$$\sigma_\theta = \frac{ps}{h}\tan(\alpha) \qquad \sigma_s = \frac{ps}{2h}\tan(\alpha) \qquad u_r = \frac{ps^2 \sin(\alpha)\tan(\alpha)}{2Eh}(2 - v)$$

Where:

σ_θ = hoop stress

σ_s = meridional stress

u_r = radial displacement

p = internal pressure

s = path from the tip of the cone down the outer cone surface

h = uniform thickness of the shell

α = angle from outer surface to centerline

E = Young's modulus

v = Poisson's ratio

The radial displacement, hoop stress, and meridional stress equations were then used as the theoretical solutions for simulation result comparisons. In order to compare results, first, a model needed to be created that best reflected the theoretical situation. A model was tested within Abaqus that matched as closely to the theoretical description as possible. This model was a simple cone without the blunt nose. It was modeled as a shell, whose thickness was added later by Abaqus. Several parameters where chosen within Abaqus that allowed the model to best reflect the theoretical results.

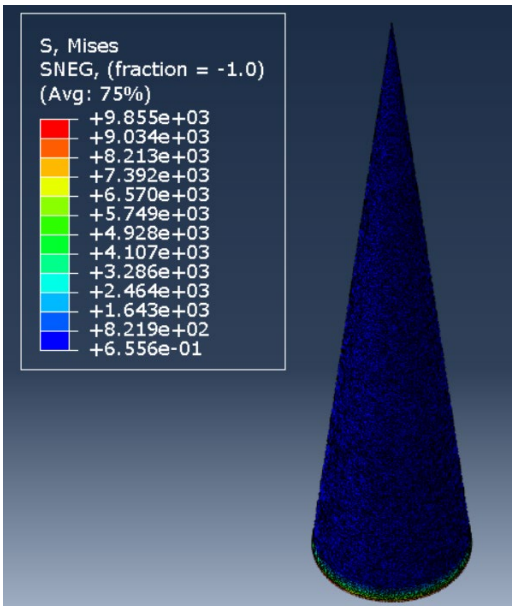

Figure 5 Abaqus straight cone membrane model

Boundary conditions

The first consideration was given to the boundary conditions of the model. Initial boundary conditions chosen strongly influence results.

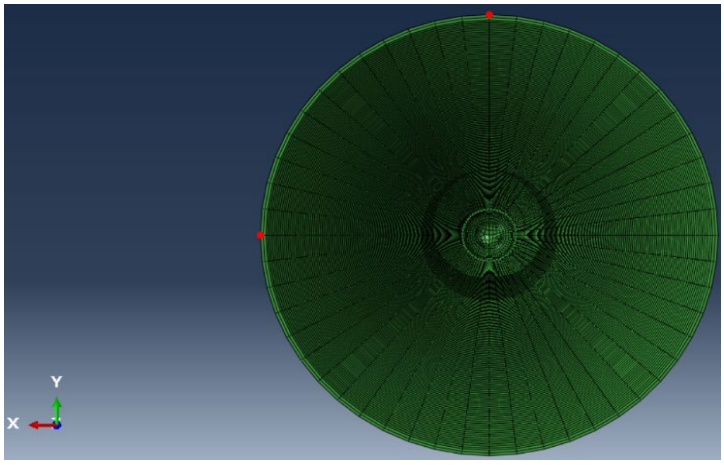

Figure 6 X-symmetry Y-symmetry Node constraints

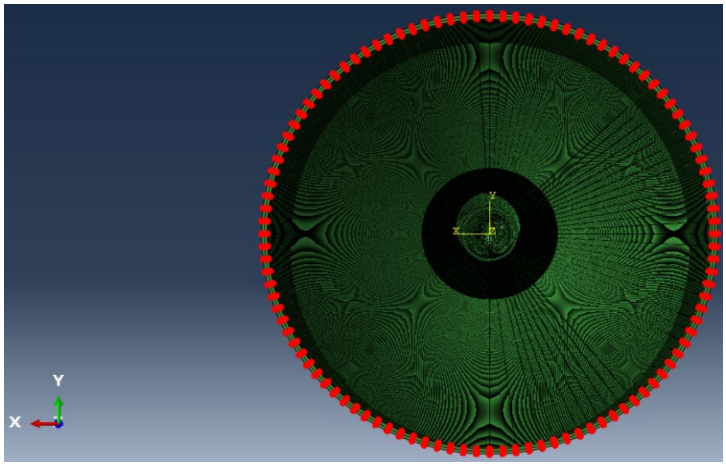

Figure 7 Z-symmetry Node constraints

Figure 6 depicts the bottom side of the nose cone as if one were peering into it. The two nodes highlighted in red are ones that have been constrained. The node on the x-axis is

constrained using y-symmetry meaning it cannot move or rotate around the y-axis. Similarly, the node on the y-axis is constrained with x-symmetry. Figure 7 shows a ring of nodes that were constrained using z-symmetry.

Those boundary conditions resulted in some strange results from the solver, such as displacements that were not symmetric around the z-axis. Other boundary conditions with constrained nodes resulted in stress concentrations and other undesirable effects.

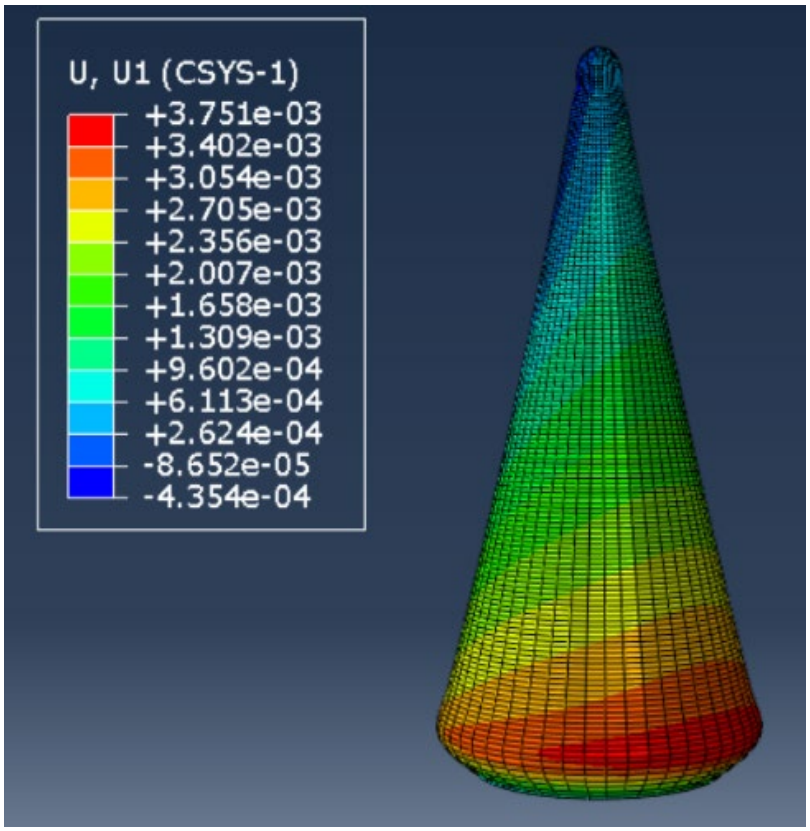

Figure 8 Asymmetric radial displacement readings

Inertia Relief was used to avoid some of the disadvantages of more traditional boundary conditions for the model. Inertia relief is a way for Abaqus to use the models inertia as a means of keeping the model in equilibrium while remaining unconstrained. This eliminated any stress concentrations that were in place as an artifact from any poorly defined boundary conditions, and made for uniform stresses, and displacements around the cones z-axis. A plate was added in on

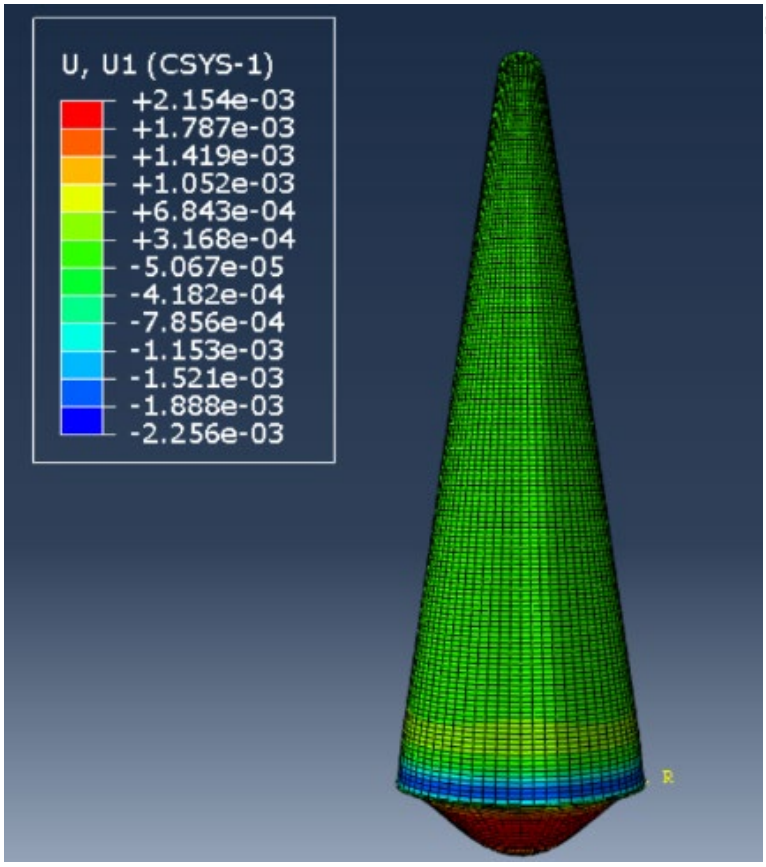

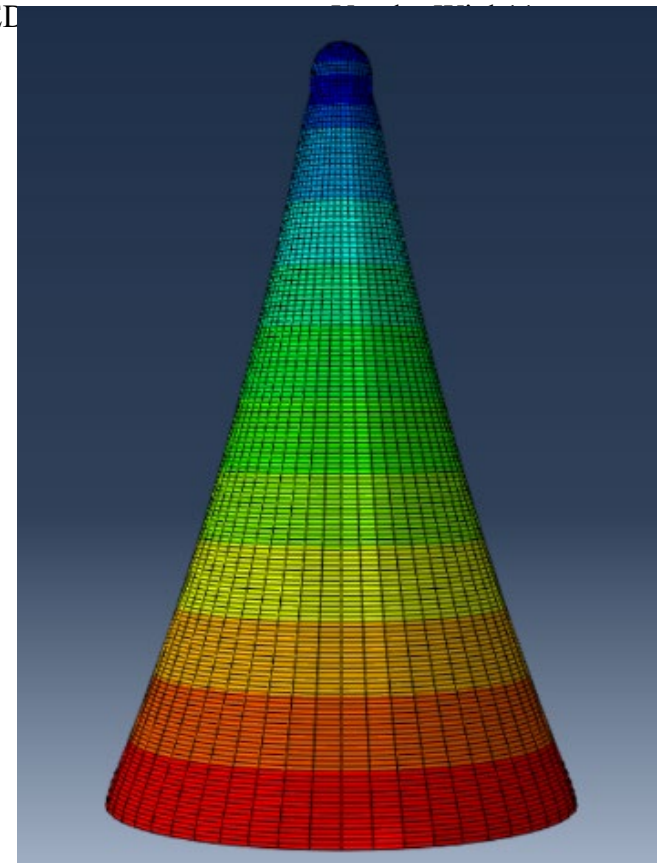

the aft section of the cone. This appeared to be required by the theoretical solutions, but was overlooked through the first several attempts at matching the theory.

Metric path definitions

Other considerations included the path definition. The theoretical solution describes a path (*s*) which begins at the tip of the cone and continues down the outer surface of the cone. In the model, paths were defined a distance below the start of the semi-spherical tip of the nose cone, since that section of the cone was known already not to match the theoretical solutions due to the differences in geometry. In fact when considering meridional stress is defined with respect to the surface of the conic body, the coordinate system for measuring meridional stress would be required to change with the curvature of the blunt tip. The differences in path definition required

Figure 10 Inertia relief with base plate

Figure 9 Inertia relief excluding baseplate

a starting distance to be added to all the data sets. The result was data that appeared to have been shifted.

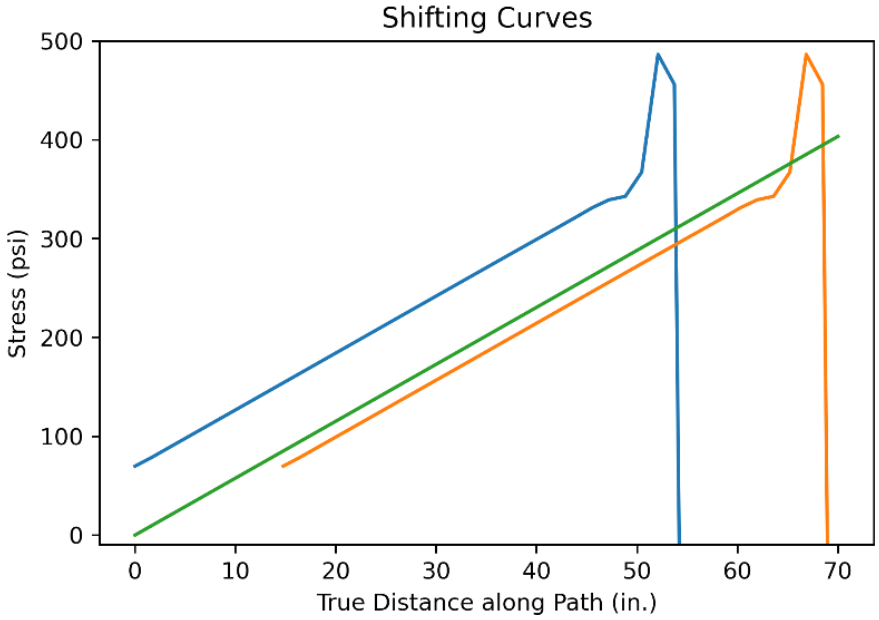

Figure 11 Hoop stress data being shifted (blue to orange) compared to the theoretical (green)

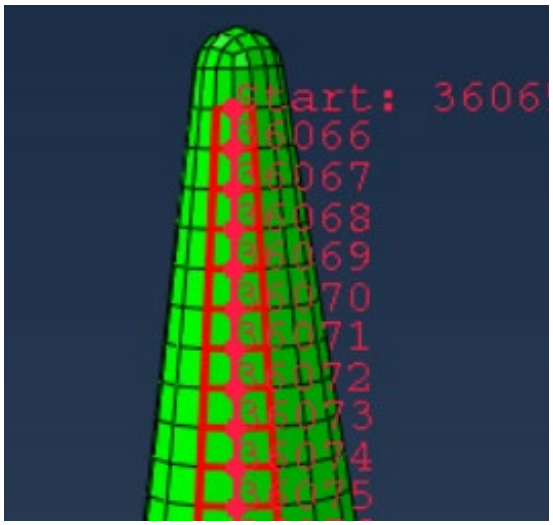

Figure 12 Path Definition

Mesh refinement

The method for mesh refinement was chosen to use a CUBIT inbuilt function that allowed for hexahedral mesh elements to be split into eight octants. This allowed for consistent path definitions between different mesh densities and allowed for regular increases in the refinement of the mesh. Two final parameters were chosen in Abaqus to help with the possibility of bending in the model. First, all of the mesh densities were assigned enhanced hourglass control that helps elements experiencing large displacements to help them avoid twisting in a non-physical fashion. Second, nonlinear geometry was used to better predict displacements in membrane models with small-strain assumptions to yield larger displacements.

Results and discussion:

Error analysis

Starting with the simplest form of the model, a membrane cone was tested that modeled the theoretical solutions as closely as possible.

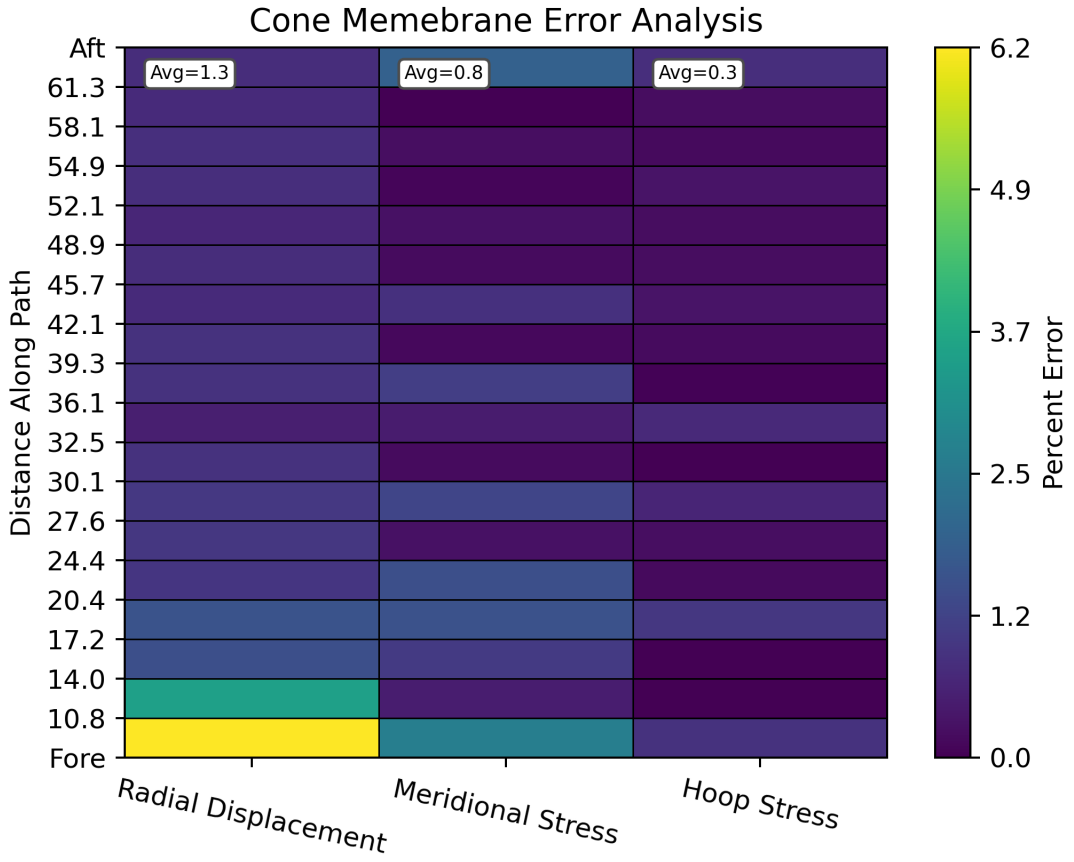

Figure 13

Figure 13 is a heat map with color showing percent error when comparing the theoretical results with the membrane model. The vertical axis is distance along the path (s) as defined by the theory. The path was defined starting a distance below the tip of the cone. Similarly, the aft section of the cone was excluded from the results since there is known to be a stress concentration near the sharp edge that the closure plate creates with the body of the cone, which is not covered by the pressure vessel theory.

Errors were taken at each point defined along the path and the results matched the theoretical solution very closely as shown in Figure 13, with average errors for hoop and meridional stresses at 0.3 and 0.8 percent respectively. The radial displacement averaged 1.3 percent error along the chosen path. Averages were taken along each column of the plot and are presented at the top of the column. The mesh used for this model was very fine, with 42,876 two dimensional elements, giving some level of confidence that the same parameters would be useful when applied to the more complex nose cone geometries.

When considering the more complex geometry of the nose cone, similar results are seen. The nose cone sees higher errors, but this is also expected because of the difference in geometry between the nose cone and the theory used for comparison.

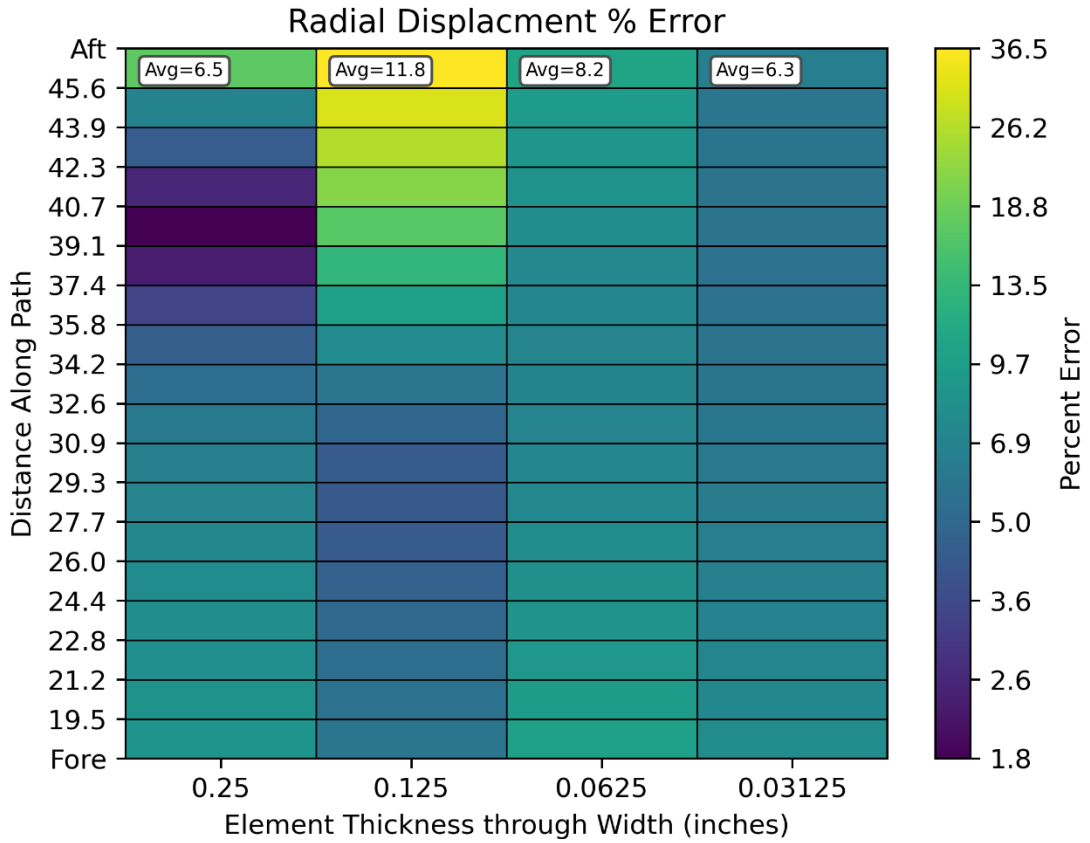

Figure 14

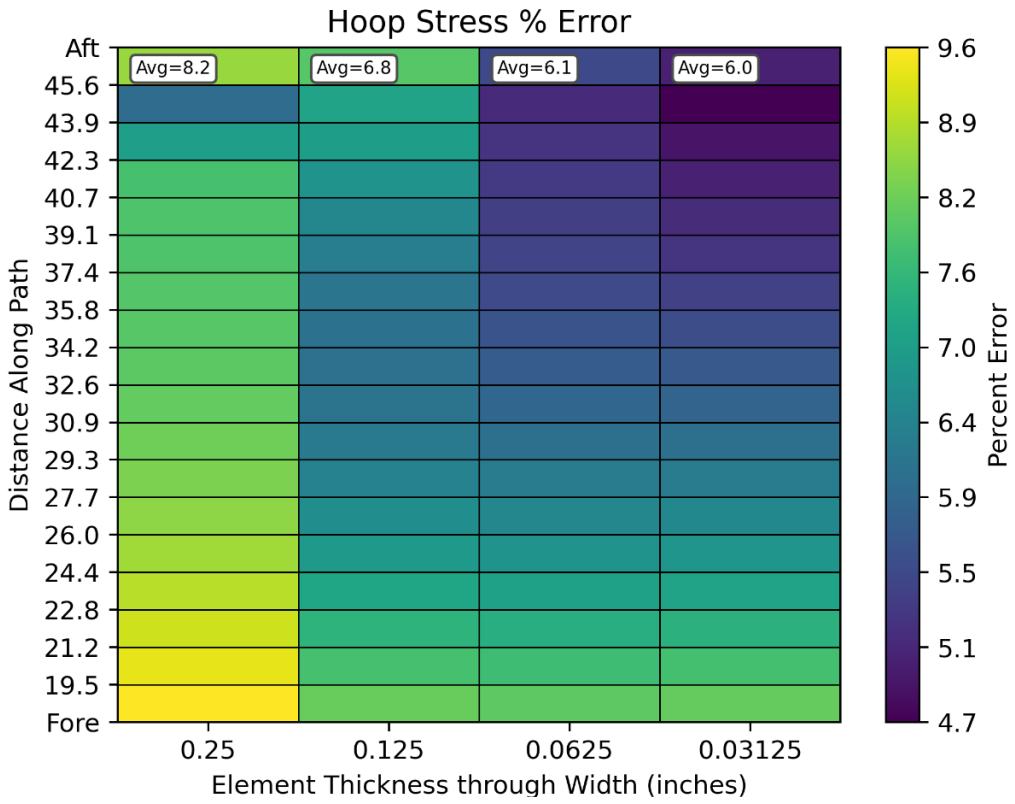

Figure 15

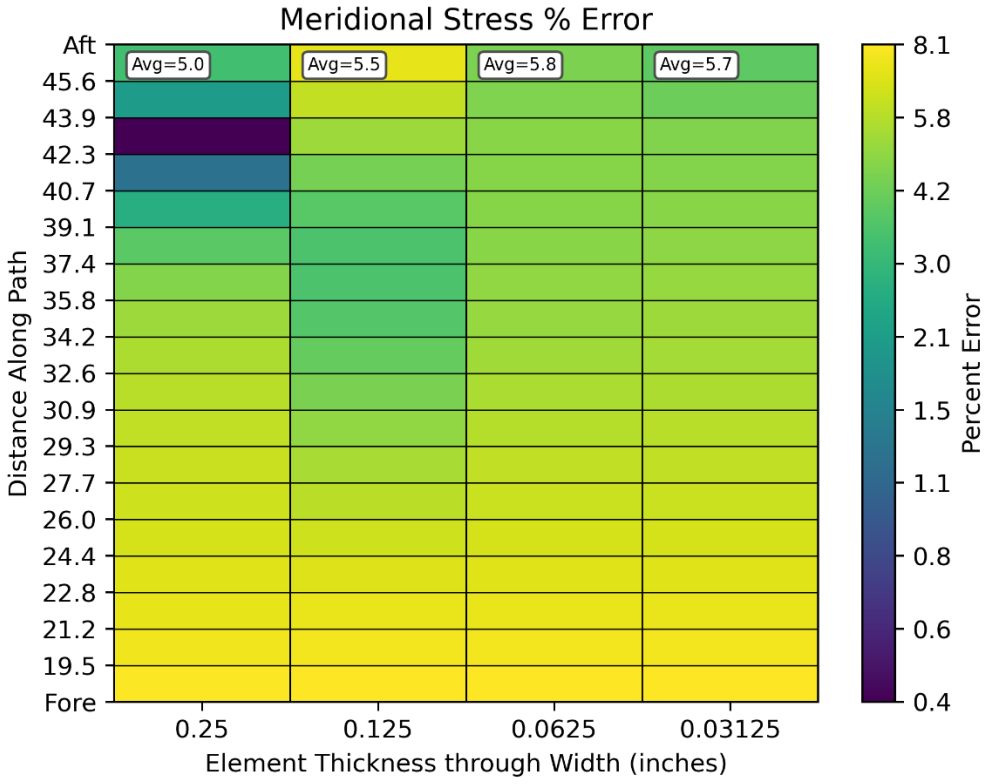

Figure 16

In Figures 14, 15, and 16, percent error between the theoretical solution and the models run is along the path (*s*) defined in Abaqus. Each column represents a finer mesh density from left to right. Another way to think about the mesh density would be the number of elements through the thickness of the nose cone with the coarsest mesh containing one element through the thickness, followed by 2, 4 and 8 elements. The color scale is logarithmic. Looking at the 0.0625 and 0.03125 element thicknesses, Figures 14, 15, and 16 appear to show that the mesh has begun to converge upon a result, with individual points along the path looking very similar from one mesh to the next as well as the averages being very comparable.

When looking at how the averages compare from coarsest mesh to finest, it seems strange that the progression does not appear to strictly decrease. One possible explanation for this phenomena comes from the path definition. Looking more closely at the coarsest mesh shows that there is some asymmetry radially around the surface of the cone. The path definition seems to pass right through as stress hot spot that occurs, likely as an artifact of how the cone was meshed resulting in higher stress and displacement values. This is reflected when looking at around 37-45 inches along the path with respect to the coarsest mesh. In all cases the error is very low in this range. As the mesh is further refined, these localized errors seem to normalize with respect to error elsewhere along the path.

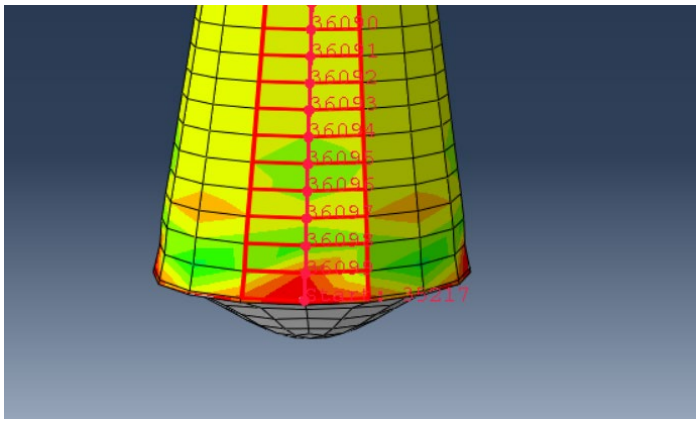

Figure 17 Coarse mesh dissymmetry along path

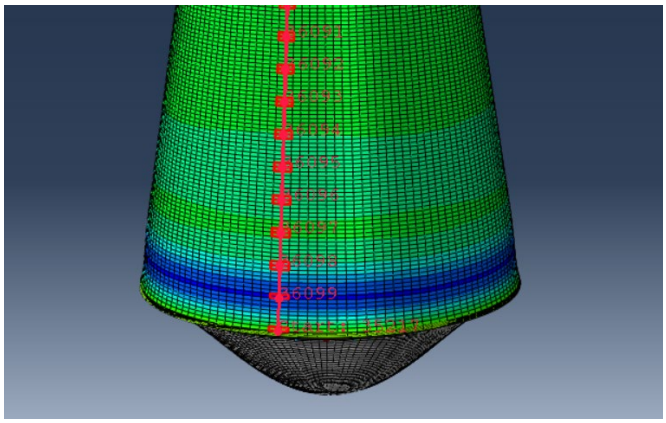

Figure 18 Fine mesh symmetry along path

The image on the left showing obvious lack of radial consistency in the coarsest mesh picked up by the path definition. The image on the right showing how finer meshes eradicated any localized hot spots. A radial average of all paths possible along the cone could have been calculated, however to be consistent with the theoretical solution, this was not considered.

Finally, other element types were tested to see what effect these would have on overall accuracy. The C3D8I element type was tested and compared to prior results.

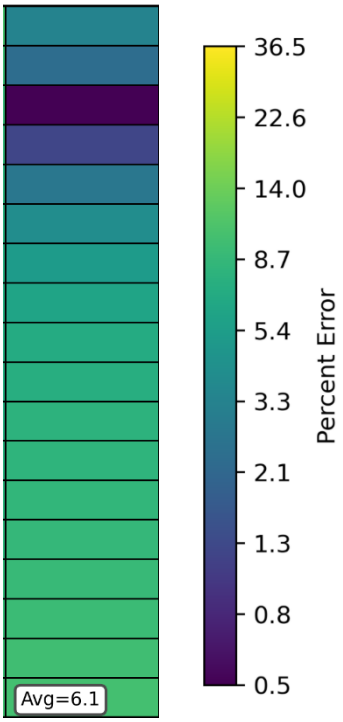

Figure 21 Radial displacement error for the C3D8I element type

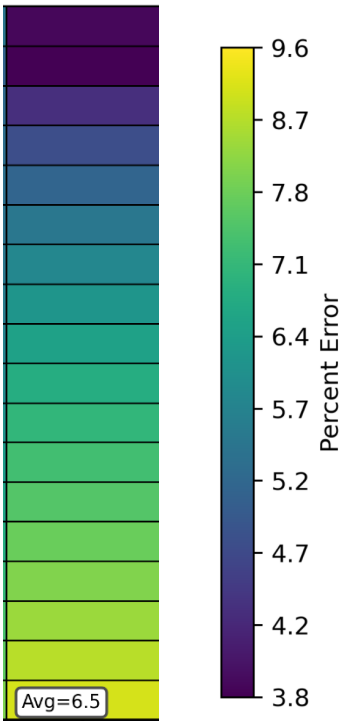

Figure 19 Hoop stress error for the C3D8I element type

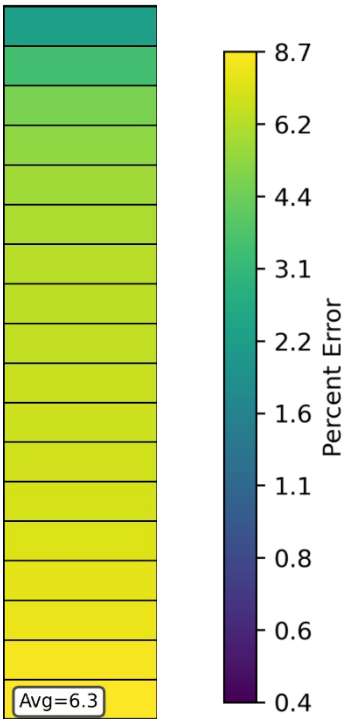

Figure 20 Meridional stress error for the C3D8I element type

Figures 19, 20, and 21 depict the C3D8I element type that does better under bending conditions than the traditional C3D8R element type used in prior simulations. The C3D8I element removes shear locking and "volumetric locking is much reduced" (Abaqus 2016 documentation). The bending issue is resolved to some extent by using the C3D8I element. Figures 19, 20, and 21 show greatly reduced errors near the aft plate, where the greatest amount

of bending was experienced. When changing element types, an element that tends to perform very well in one area tends to underperform in other areas. This can be seen in near the fore of the nose cone where error is relatively high, and bending is the least of the concerns. Higher order elements may be used in the future to as a means of eliminating some of the restrictions experienced by the C3D8I elements while still getting the benefits of decreased error in the aft end.

Overall, with the high correlation between the theoretical and the membrane cone model, there is reason to believe that the blunt tipped nose cone model is very close to modeling a physical object. However with the error increasing with mesh density in some cases, questions seem to be raised. One possible explanation for this would be that as the mesh becomes more refined, the Abaqus solver is encountering new physics in the geometry of the cone. However a finer mesh density would be needed to determine if the error would continue to decrease, but computing power was not available to carry out such an experiment.

Pressure Mapping:

Having some measure of confidence in the fidelity of the nose cone mesh, an external pressure was applied to the surface of the nose cone. This pressure time-history data used in mapping was generated from a CFD simulation that modeled an air blast test done in LANL facilities. Using a suite of Python mapping scripts provided by Paula Rutherford, pressure was linearly interpolated from the pressure gauge locations onto elements in between.

With the pressure being interpolated onto each element of the nosecone, an Abaqus simulation could be run with the pressure data being the loading condition. The Abaqus simulation allowed results for stresses, displacements, and rigid body motion, to see how the conic body reacted to the pressure wave.

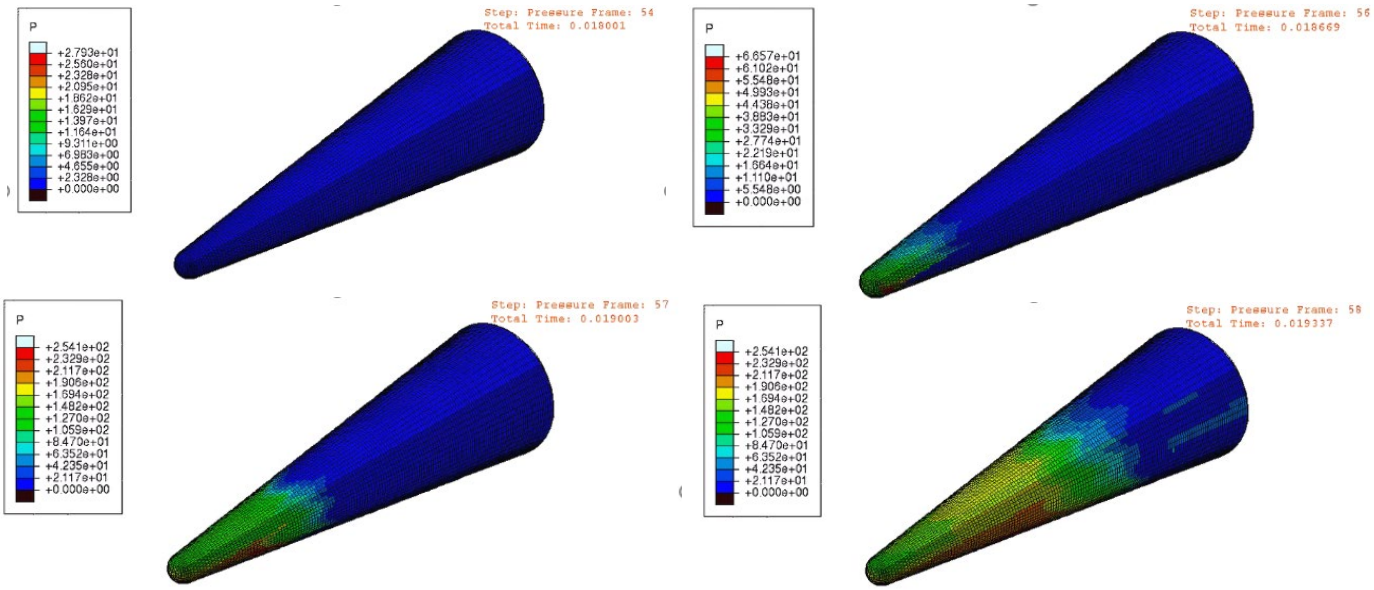

Figure 22 Pressure wave applied externally

The pressure wave can be visualized by a series of frames. Figure 22 depict the very start of the pressure wave as it travels down the length of the cone, and with enough frames, a movie could be stitched together to visualize how pressure is applied to the surface of the cone through time.

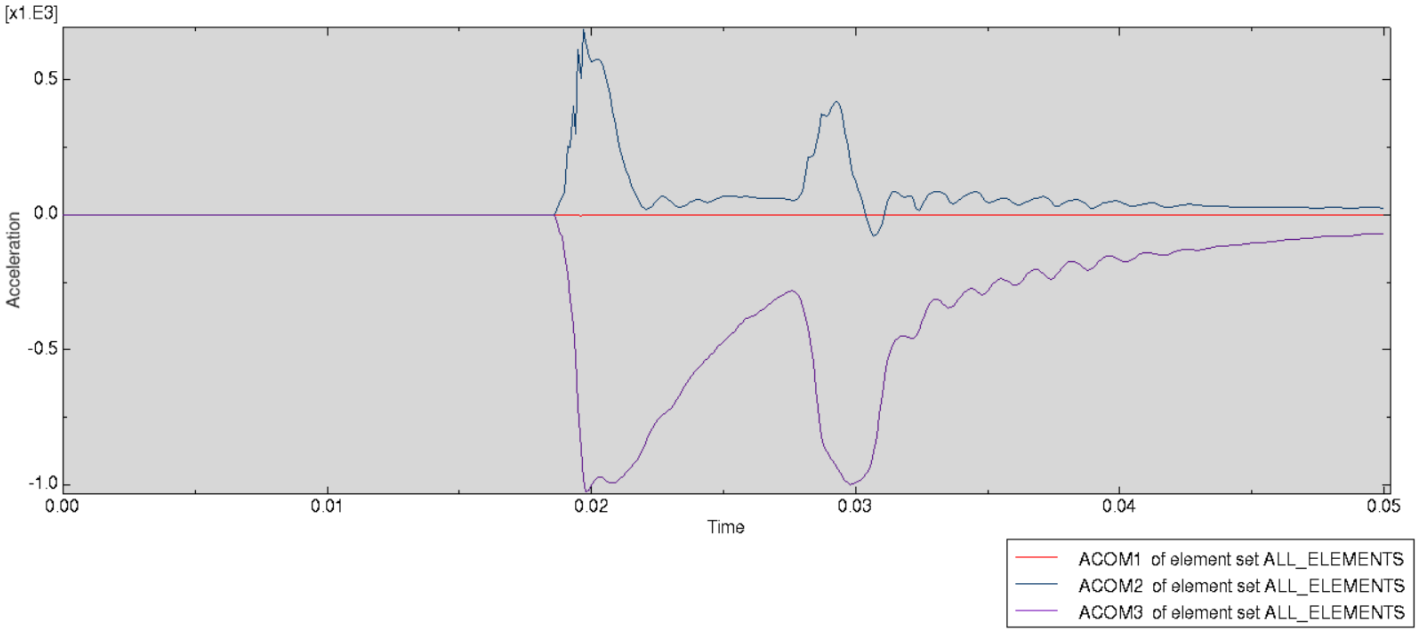

Figure 23 Acceleration in X, Y and, Z directions depicting rigid body motion

This pressure wave produced rigid body motion from surface integration. Taking a look at the acceleration one can determine in what directions the body is moving after being hit by the pressure wave. The blue line refers to acceleration in the y-axis, which can be seen to be moving in the positive direction, or upwards with respect to the nose cone orientation in prior frames. The purple refers to the z-direction, and is negative, indicating that the nose cone is moving backward. The red line sees nearly no change indicting almost no motion in the x-direction.

With these mapping capabilities, much more information can be ascertained from the pressure data. This pressure data can help researchers understand flight characteristics and the strength of the nose cone under external pressures endured in a blast environment.

Next Steps:

Further research will be conducted on the particular flight characteristics of this nose cone its response to the blast environment. A parameter study will be used to understand their effects on the nose cone, such as geometry, material properties, and the environment.

The current mapping scripts are slow due to the complexity of the interpolation method. A nearest neighbor interpolation method will be developed that will likely be faster than the linear method. Comparisons will be drawn between the linear and nearest neighbor methods to determine if the accuracy sacrificed for speed is worthwhile.

Conclusion:

Building simulations and models in an FEA solver is often useless without confirmation that the models being build are accurately modeling a physical object. By comparing to theoretical solutions, there can be some measure of confidence that meshed models are not providing junk data. Additionally, mesh sensitivity can be used to weigh computational cost with accuracy of models, and determine what mesh density is required for all different types of

problems. The nose cone geometry used in this study was compared to theoretical internally loaded pressure vessels and found to match relatively well to these closed-form solutions. Additionally, the model was found to be converging around the third or fourth finest mesh density. Unfortunately, a finer fifth mesh was unable to be tested to confirm that the results would continue to decrease. With confidence in the mesh accuracy, pressure-time history data was applied to the external surface of the cone giving analysts the ability to ascertain structural characteristics and flight characteristics about the model.

Bibliography:

Au, Norman N. “Stresses in Thin Vessels Under Internal Pressure.” Aerospace Corporation, Approved by J. Steinman, Department of Defense 15 Jan, 1964.

Ghurlston, Robert. “What Is Nonlinear Geometry in Fea? And When Should You Use It?” *Fidelis*, Fidelis, 1 Apr. 2021, www.fidelisfea.com/post/what-is-nonlinear-geometry-in-fea-and-when-should-you-use-it.

Kayafas, Gus, and Harold E. Edgerton. “Bullet Shock Wave.” *Smithsonian American Art Museum*, 1988, americanart.si.edu/artwork/bullet-shock-wave-32701.